Supplement of Atmos. Chem. Phys., 25, 13863–13878, 2025
https://doi.org/10.5194/acp-25-13863-2025-supplement

Supplement of

Meteorological influence on surface ozone trends in China: assessing uncertainties caused by multi-dataset and multi-method

Xueqing Wang et al.

Correspondence to: Jia Zhu (jiazhu@nuist.edu.cn)

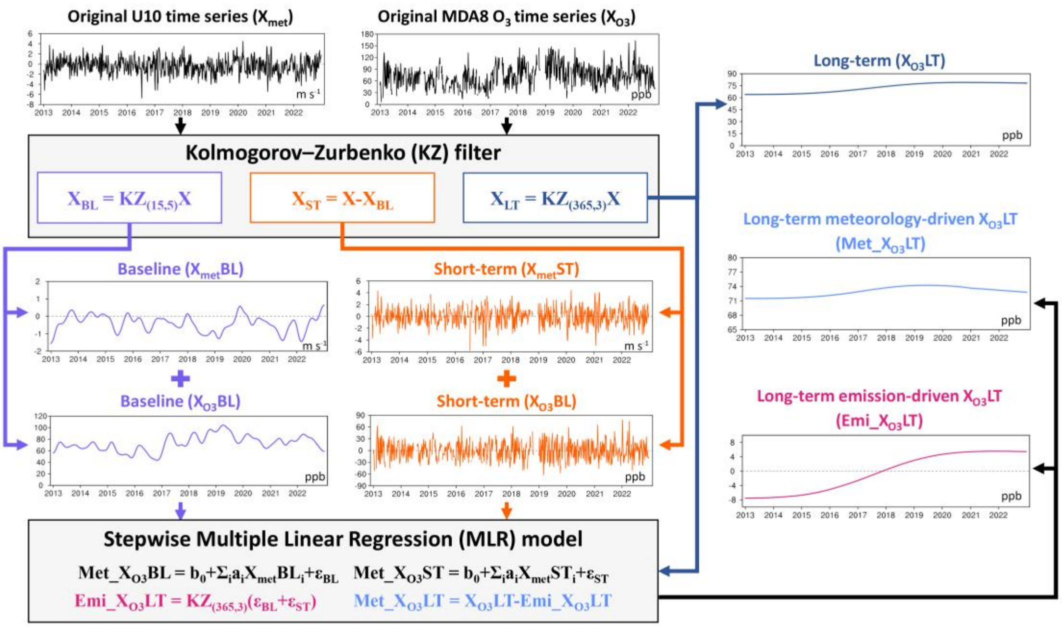

Figure S1. Flowchart of Kolmogorov-Zurbenko - Multiple linear regression (KZ-MLR) model, which decomposes the observed MDA8 O_3 time series into meteorology-driven and emission-driven long-term components. Shown on the figure is an example: MDA8 O_3 data from Station_1015A and U10 data from ERA5 during the summer.

Abbreviations:
CMA: China Meteorological Administration
ECMWF: European Centre for Medium-Range Weather Forecasts
ERA5: The fifth generation ECMWF atmospheric reanalysis of the global climate
ERA-Interim: ECMWF Reanalysis - Interim
FNL: National Centers for Environmental Prediction Final Operational Global Analysis data (1.0°×1.0°)
FNL025: National Centers for Environmental Prediction Final Operational Global Analysis data (0.25°×0.25°)
MERRA2: Modern-Era Retrospective analysis for Research and Applications Version 2
KZ: Kolmogorov–Zurbenko filter
MLR: Multiple Linear Regression
RF: Random Forest
XGBoost: eXtreme Gradient Boosting
LightGBM: Light Gradient Boosting Machine
Lowess: Locally Weighted Linear Regression
GEOS: Goddard Earth Observing System
WRF: Weather Research and Forecast
CMAQ: Community Multiscale Air Quality
WRF-Chem: WRF model coupled with Chemistry
RegCM-Chem-YIBs: Regional Climate-Chemistry-Ecology Coupling Model
NCP: North China Plain
BTH: Beijing-Tianjin-Hebei Region
YRD: Yangtze River Delta Region
PRD: Pearl River Delta
SCB: Sichuan Basin
FWP: Fenwei Plain
THB: Twain-Hu Basin

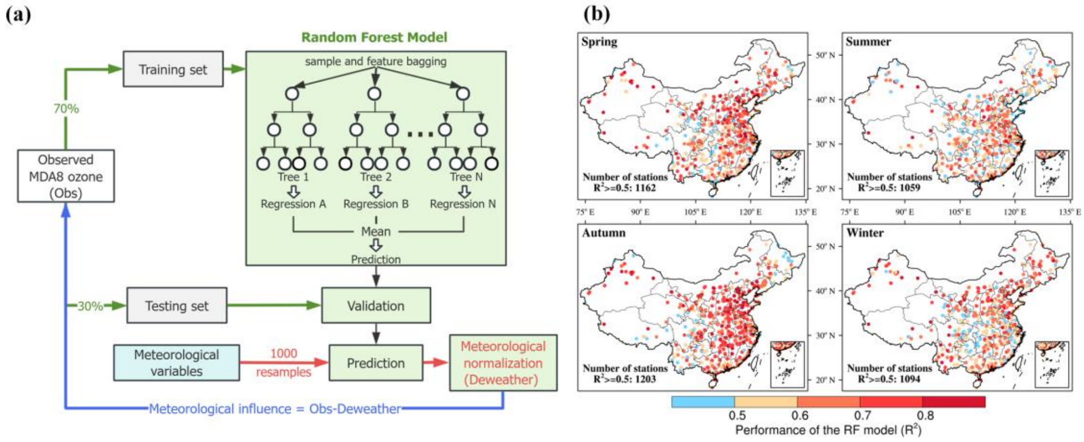

Figure S2. (a) Conceptual diagram of obtaining the meteorological influence based on the Random Forest (RF) algorithm, and (b) the performance of the RF model for the testing dataset at each state-controlled station during four seasons. The number of state-controlled monitoring stations with the coefficient of determination (R^2) greater than or equal to 0.5 is also presented.

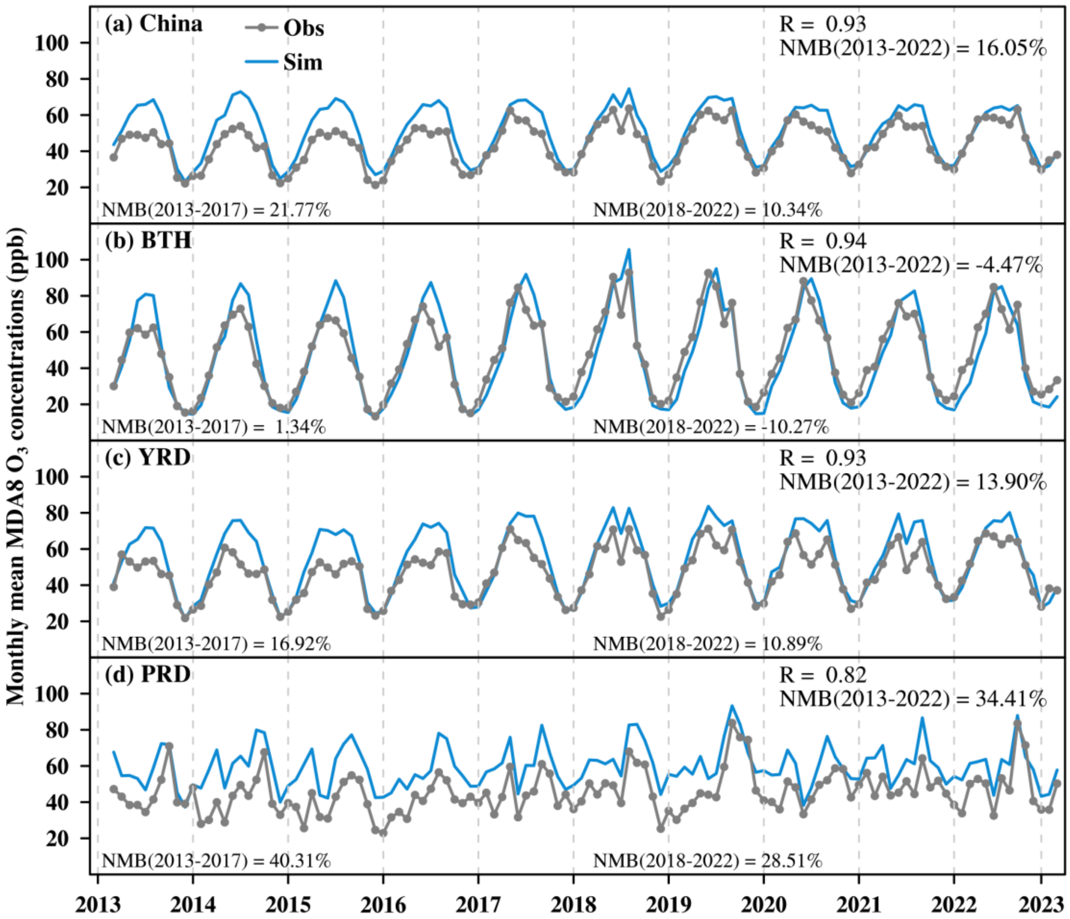

Figure S3. Comparison of simulated (blue) and observed (grey) monthly mean MDA8 O_3 concentrations averaged over (a) China, (b) BTH, (c) YRD, and (d) PRD from 2013 to 2022. The correlation coefficient (R) and normalized mean bias (NMB) values are shown. The NMB for 2013–2017 and 2018–2022 are also calculated and shown in order to test the performance of GEOS-Chem at different time periods.

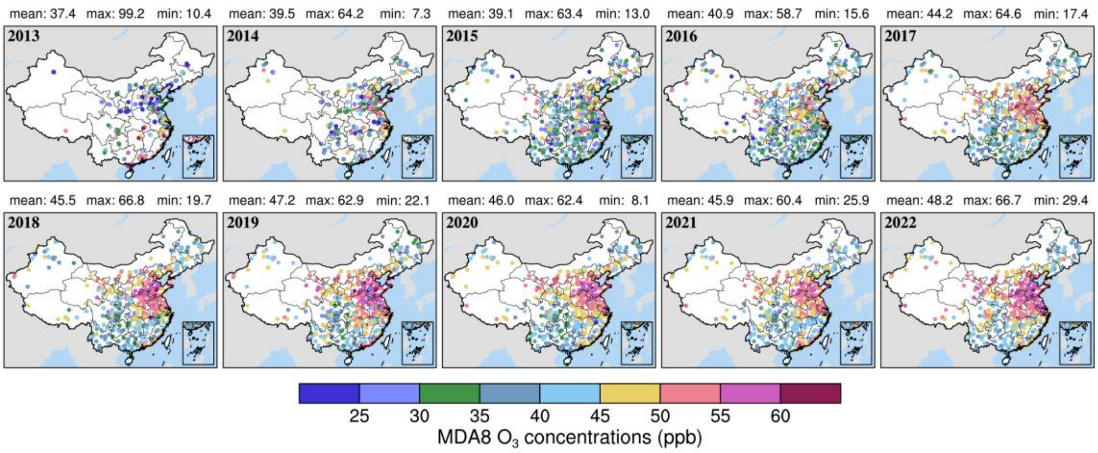

Figure S4. Annual mean MDA8 O_3 concentrations in China from 2013 to 2022. The mean, maximum, and minimum MDA8 O_3 concentrations for the whole China are shown.

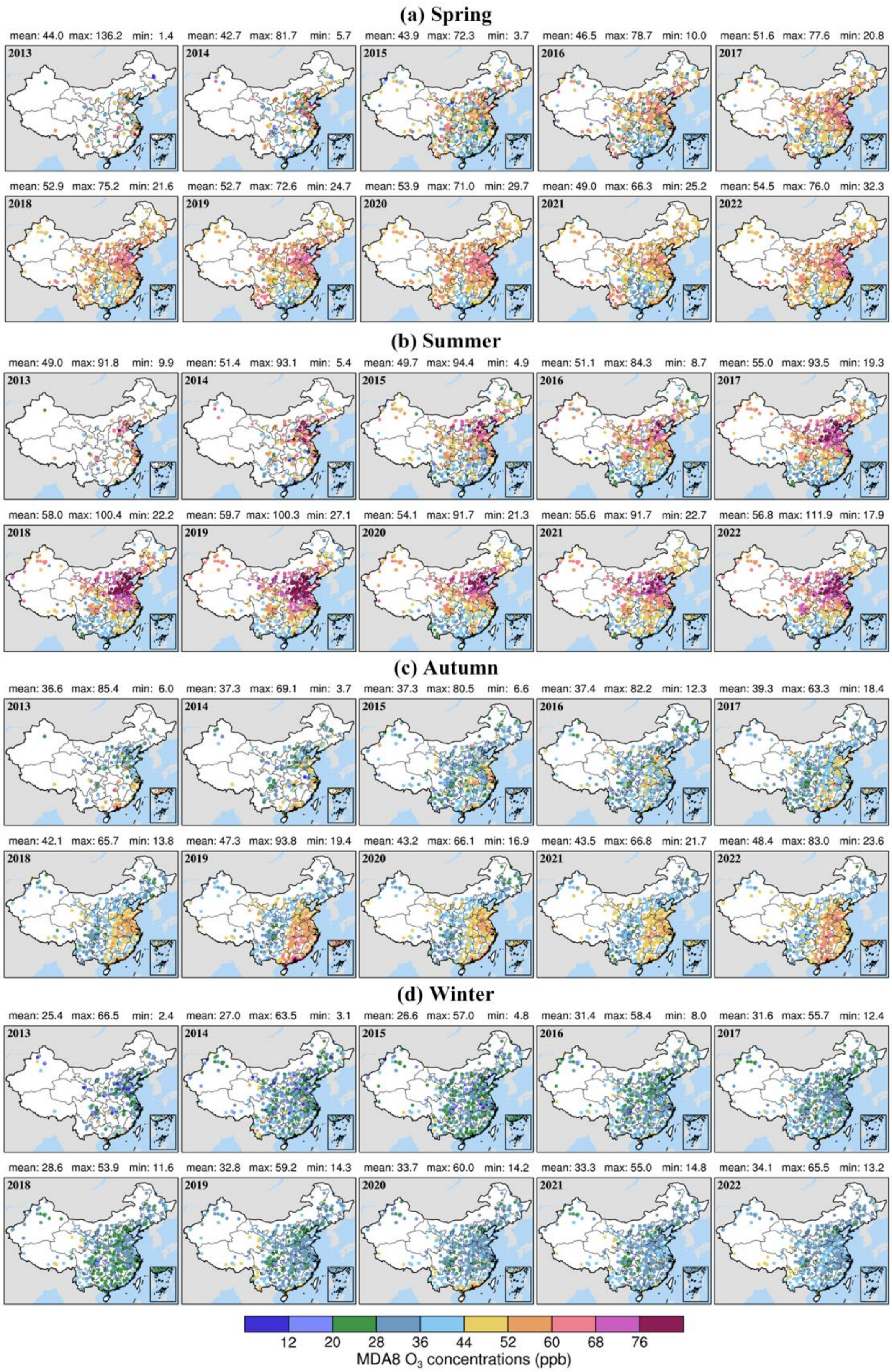

Figure S5. Seasonal mean MDA8 O_3 concentrations in China during (a) spring, (b) summer, (c) autumn, and (d) winter. The mean, maximum, and minimum MDA8 O_3 concentrations for the whole China are shown.

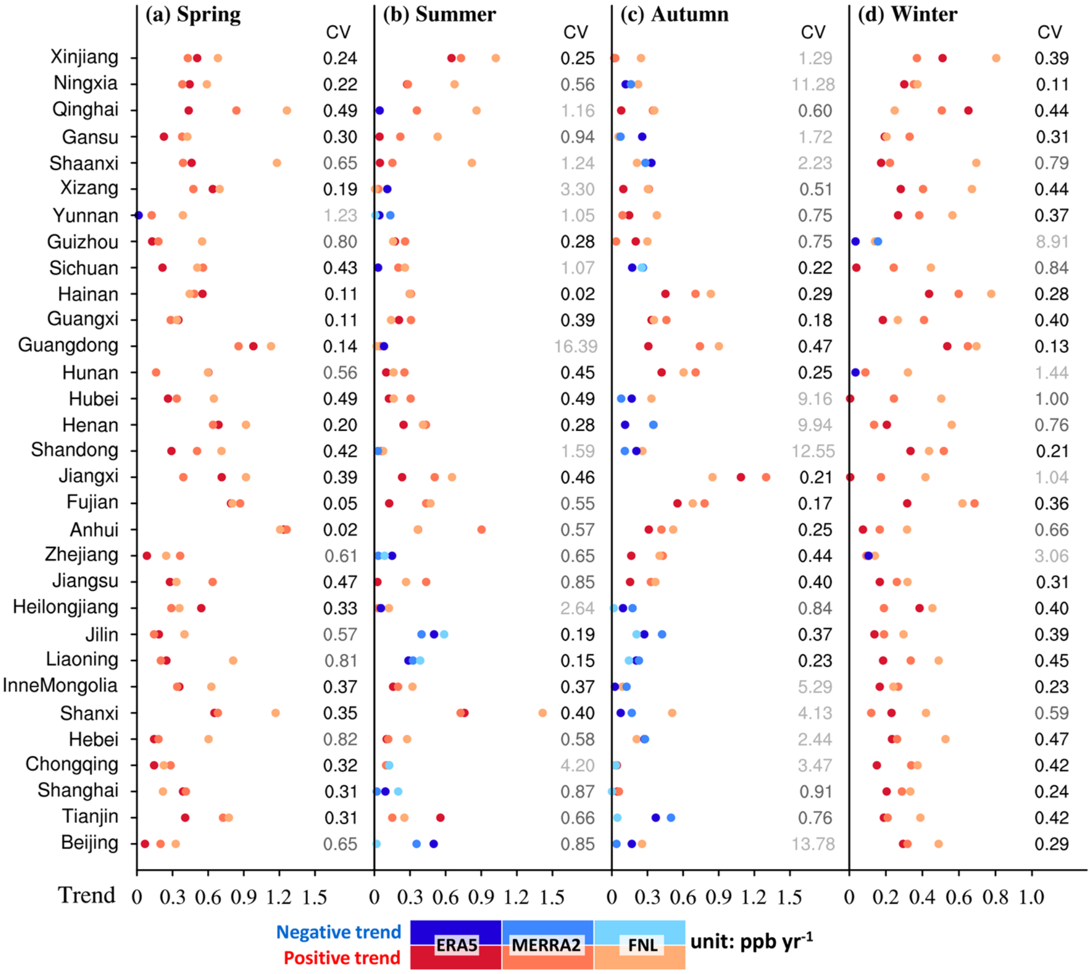

Figure S6. Trends in meteorology-driven MDA8 O_3 concentrations calculated by ERA5-, MERRA2-, and FNL-driven MLR models in China's 31 mainland provinces during (a) spring, (b) summer, (c) autumn, and (d) winter. Markers in red and blue represent the positive and negative trends, respectively. The absolute value of the coefficient of variation (CV) is shown. The CV is calculated by the standard deviation of trends derived from ERA5-, MERRA2-, and FNL-driven MLR models divided by the mean. The darker colour means the lower uncertainty in quantifying the meteorological impact on observed O_3 trends.

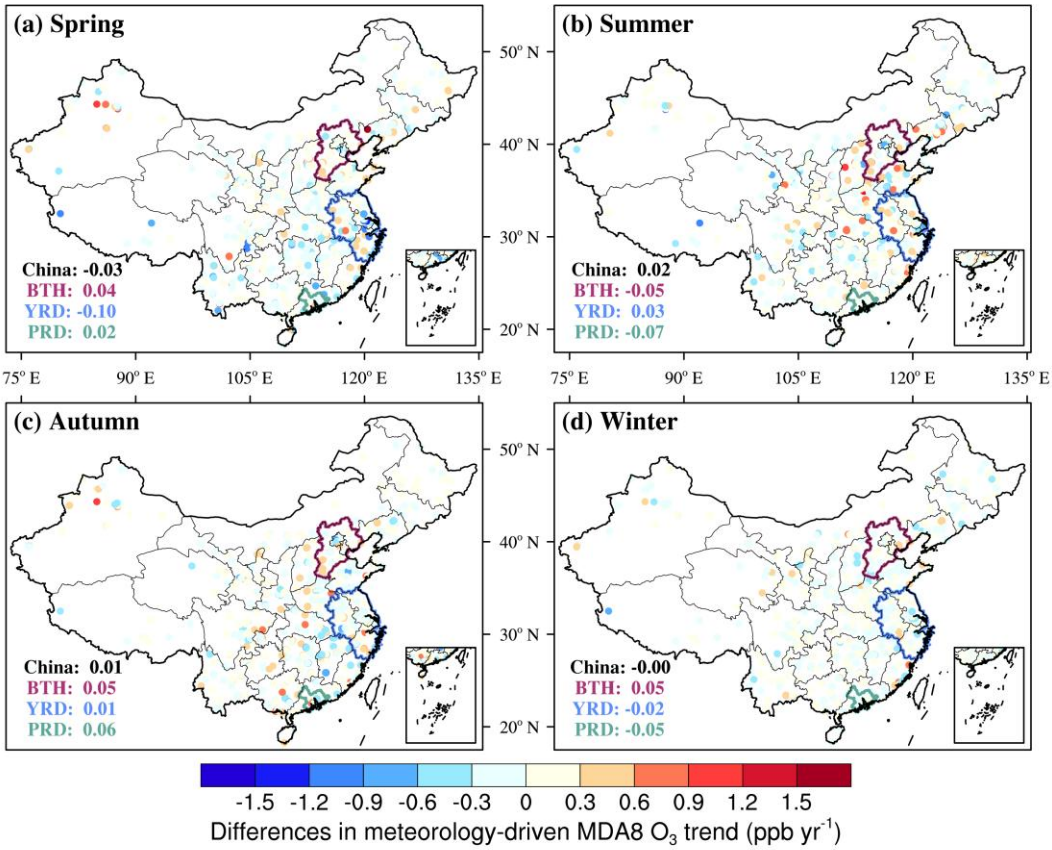

Figure S7. Differences between meteorology-driven MDA8 O_3 trends calculated by FNL- and FNL025-driven MLR models in China during (a) spring, (b) summer, (c) autumn, and (d) winter. Values in black, purple, blue, and green represent the average difference for the whole China, BTH, YRD, and PRD, respectively.

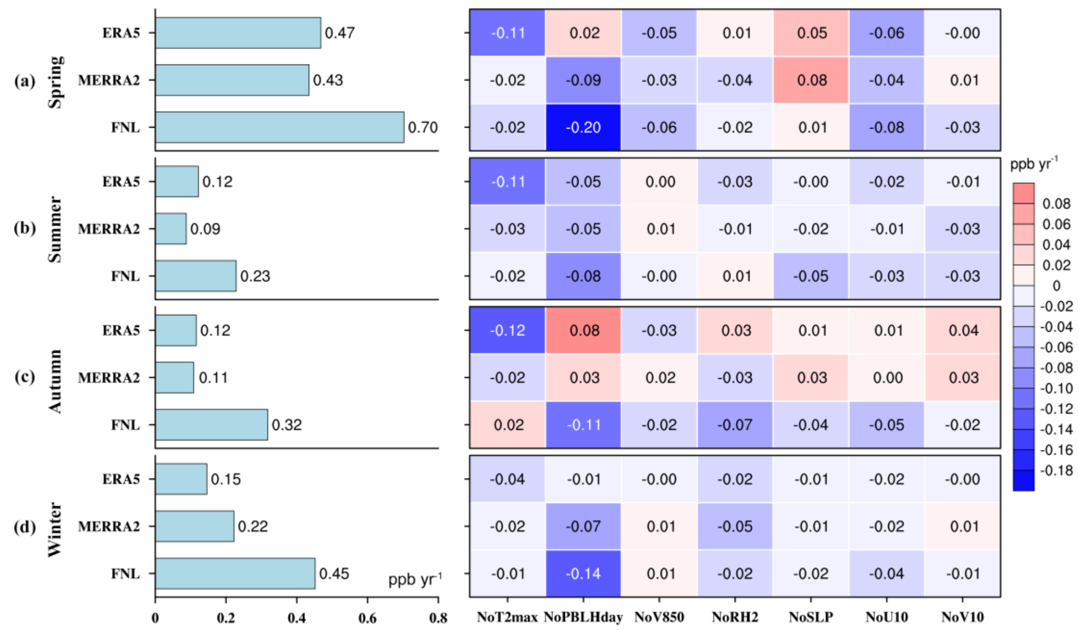

Figure S8. Construction of a multiple linear regression (MLR) model using seven common meteorological variables (i.e. T2max, PBLHday, V850, RH2, SLP, U10, V10) from ERA5, MERRA2, and FNL to quantify the meteorological influence on the MDA8 O_3 trends during (a) spring, (b) summer, (c) autumn, and (d) winter. Bars on the left represent the meteorology-driven O_3 trends derived from the three data-driven MLR models. The heatmap on the right represents the difference between the results obtained by constructing an MLR model after removing a certain meteorological variable in sequence.

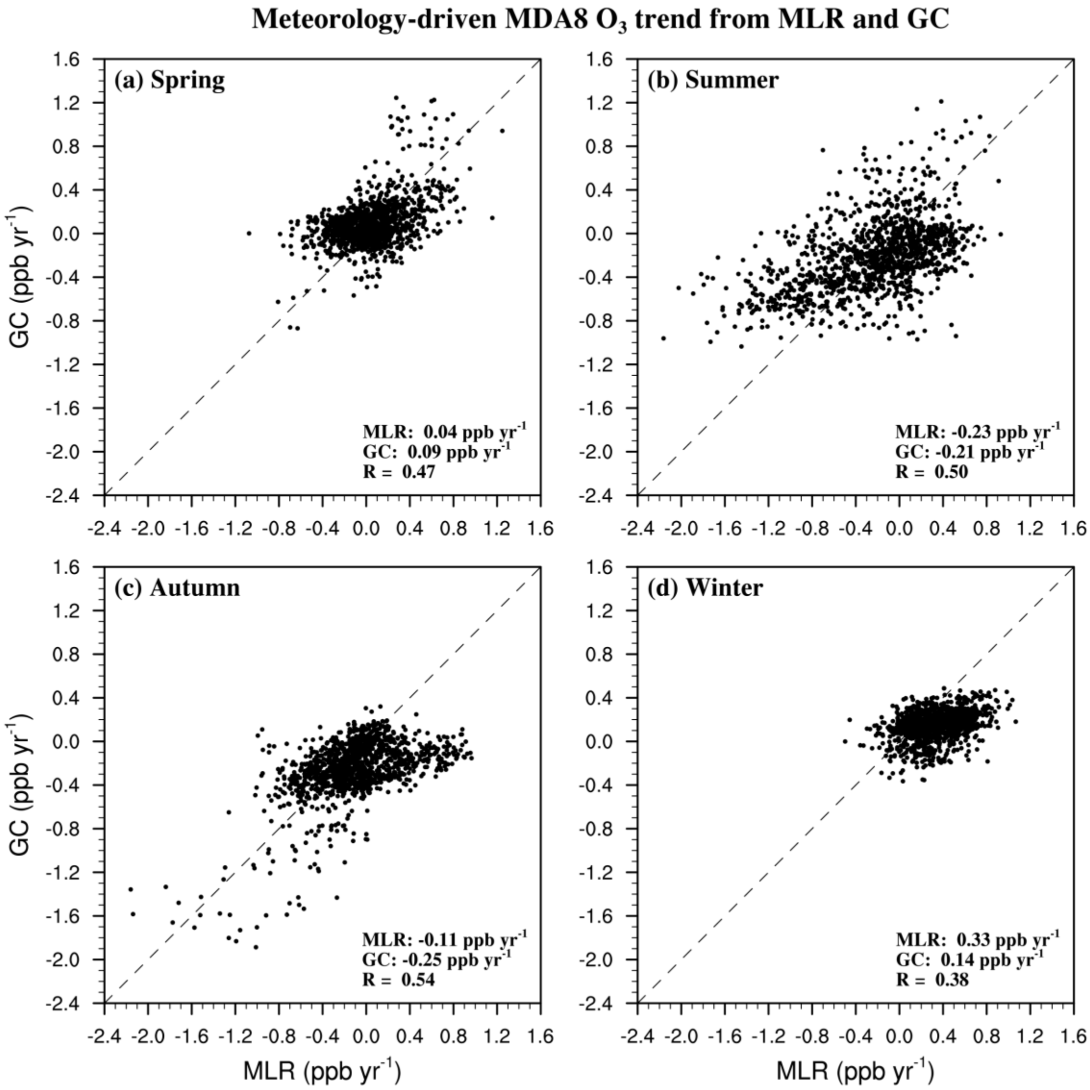

Figure S9. The comparison of meteorology-driven O_3 trends from the MERRA2-driven multiple linear regression (MLR) vs. GEOS-Chem (GC) models averaged over China for 2018–2022 during (a) spring, (b) summer, (c) autumn, and (d) winter. The dashed line is a 1:1 line. The coefficient of correlation (R) is also shown.

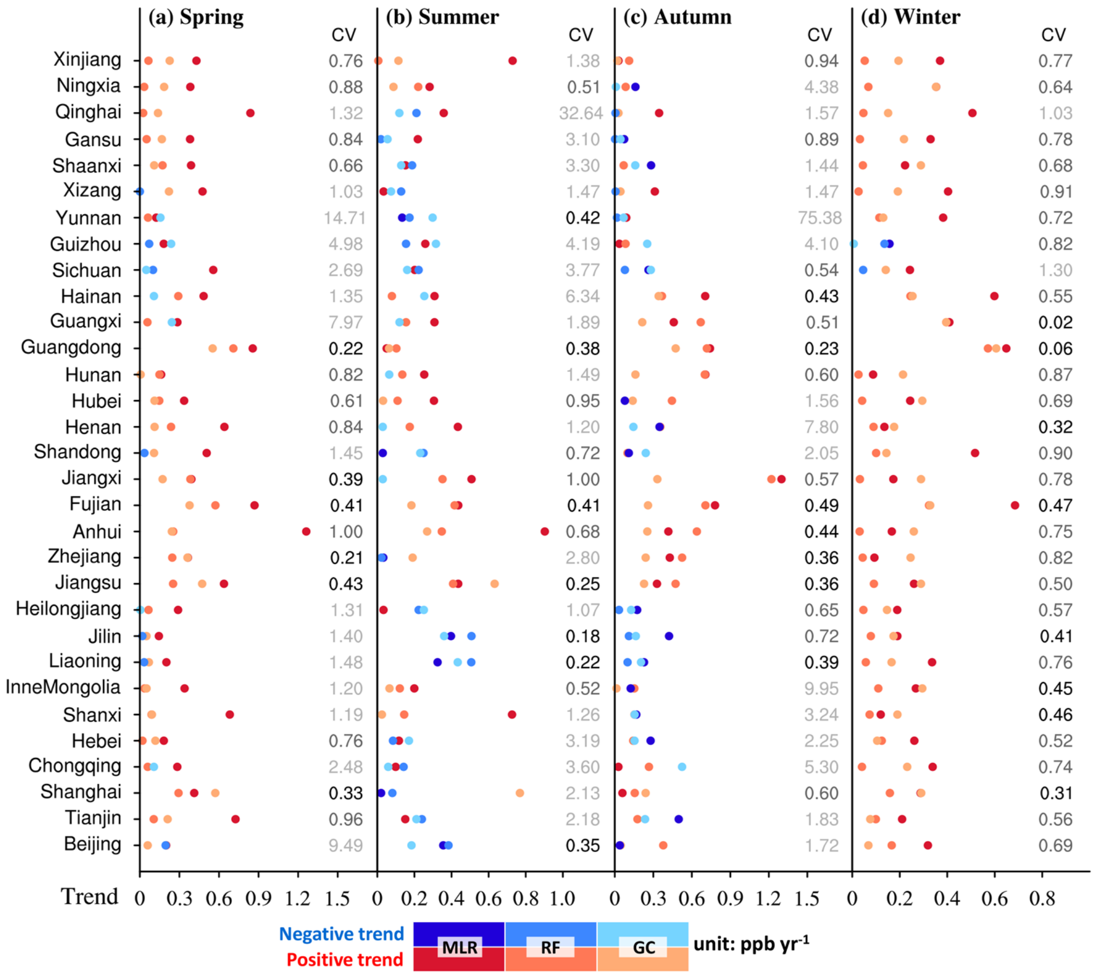

Figure S10. Trends in meteorology-driven MDA8 O_3 concentrations calculated by multiple linear regression (MLR), random forest (RF), and GEOS-Chem (GC) models in China's 31 mainland provinces during (a) spring, (b) summer, (c) autumn, and (d) winter. Markers in red and blue represent the positive and negative trends, respectively. The absolute value of the coefficient of variation (CV) is shown. The CV is calculated by the standard deviation of the trends derived from MLR, RF, and GC models divided by the mean. The darker colour means the lower uncertainty in quantifying the meteorological impact on observed O_3 trends.

63 **Table S1.** Reported studies using traditional statistical, machine learning, and chemical transport models to obtain the meteorological impact on surface O_3 in the past six years.

Region/City	Study period [a]	Model	Meteorological data	Meteorological impact [b]	Reference
Shanghai	2013–2017	KZ	N/A	+0.75 μg m^{-3} yr^{-1}	Yu et al., 2019
Tianjin	Spring, 2009–2015	Generalized additive model	Site observation	–1.11 ppb yr^{-1}	Yang et al., 2019a
	Summer, 2009–2015			+0.12 ppb yr^{-1}	
	Autumn, 2009–2015			–0.99 ppb yr^{-1}	
	Winter, 2009–2015			+0.06 ppb yr^{-1}	
PRD	2007–2017	KZ-MLR	ECMWF reanalysis	–0.8 μg m^{-3} yr^{-1}	Yang et al., 2019b
North China	Apr to Sept, 2013/2017	WRF-CMAQ	N/A	+0.2±1.1 ppb	Ding et al., 2019
Northeast China				+0.3±0.8 ppb	
East China				+2.0±1.7 ppb	
South China				+0.5±1.5 ppb	
China	Summer, 2013/2014	WRF-CMAQ	FNL	–3.2 ppb	Wang et al., 2019
North China				–8.7 ppb	
Northeast China				–4.5 ppb	
East China				–1.1 ppb	
South central China				–1.5 ppb	
Southwest China				–3.7 ppb	
Northwest China				–1.6 ppb	
China	Summer, 2013/2015			–1.8 ppb	
North China				–2.4 ppb	
Northeast China				–0.5 ppb	
East China				–2.1 ppb	
South central China				–4.2 ppb	
Southwest China				+0.2 ppb	
Northwest China				–0.9 ppb	

Region/City	Study period	Model	Meteorological data	Meteorological impact	Reference
Central eastern China	2003/2015	GEOS-Chem	MERRA2	+3.2 ppb	Sun et al., 2019
Eastern China	Summer, 2013–2018	MLR	FNL	+0.5 μg m^{-3} yr^{-1}	Han et al., 2020
BTH				+0.7 μg m^{-3} yr^{-1}	
YRD				+0.9 μg m^{-3} yr^{-1}	
PRD				+0.7 μg m^{-3} yr^{-1}	
Eastern China	Summer, 2013–2019	MLR	MERRA2	+0.7 ppb yr^{-1}	Li et al., 2020
NCP				+1.4 ppb yr^{-1}	
YRD				+0.7 ppb yr^{-1}	
PRD				+0.8 ppb yr^{-1}	
SCB				–0.2 ppb yr^{-1}	
China	Summer, 2013–2017	WRF-CMAQ	FNL	Meteorological changes dominated the changing rates of O_3.	Liu and Wang, 2020
NCP	2014–2018	MLR	ERA-Interim	+0.7 μg m^{-3} yr^{-1}	Chen et al., 2020
YRD				+0.7 μg m^{-3} yr^{-1}	
FWP				+0.8 μg m^{-3} yr^{-1}	
NCP	Spring, 2014–2018			+0.5 μg m^{-3} yr^{-1}	
YRD				+1.3 μg m^{-3} yr^{-1}	
FWP				+1.1 μg m^{-3} yr^{-1}	
NCP	Summer, 2014–2018			+0.8 μg m^{-3} yr^{-1}	
YRD				+1.1 μg m^{-3} yr^{-1}	
FWP				+0.8 μg m^{-3} yr^{-1}	
NCP	Autumn, 2014–2018			+1.0 μg m^{-3} yr^{-1}	
YRD				+0.8 μg m^{-3} yr^{-1}	
FWP				+1.1 μg m^{-3} yr^{-1}	

Region/City	Study period	Model	Meteorological data	Meteorological impact	Reference
NCP	Winter, 2014–2018	MLR	ERA-Interim	+0.7 μg m^{-3} yr^{-1}	Chen et al., 2020
YRD				–0.5 μg m^{-3} yr^{-1}	
FWP				+0.1 μg m^{-3} yr^{-1}	
NCP	Summer, 2012–2017	GEOS-Chem	MERRA2	+0.28 ppb yr^{-1}	Dang et al., 2021
YRD				+1.47 ppb yr^{-1}	
BTH	2015–2019	KZ-MLR	ERA5, FNL	+1.07 μg m^{-3} yr^{-1}	Mousavinezhad et al., 2021
YRD				+0.99 μg m^{-3} yr^{-1}	
PRD				+2.52 μg m^{-3} yr^{-1}	
SCB				–1.35 μg m^{-3} yr^{-1}	
Shandong	Spring, 2013/2015	WRF-Chem	FNL	+8.6%	Zhao et al., 2021
	Spring, 2013/2017			+14.5%	
	Spring, 2013/2019			+14.0%	
	Summer, 2013/2015			–7.4%	
	Summer, 2013/2017			–6.5%	
	Summer, 2013/2019			–6.2%	
	Autumn, 2013/2015			+6.9%	
	Autumn, 2013/2017			+11.6%	
	Autumn, 2013/2019			+9.6%	
	Winter, 2013/2015			–1.2%	
	Winter, 2013/2017			–0.2%	
	Winter, 2013/2019			–0.5%	
SCB	May to Jun, 2019/2020	GEOS-Chem	GEOS-FP	11.57 ppb	Sun et al., 2021
		GEOS-Chem-XGBoost		11.15 ppb	
Handan	Jun, 2013–2018	WRF-CMAQ	FNL	+2.00 μg m^{-3} yr^{-1}	Yao et al., 2021

Region/City	Study period	Model	Meteorological data	Meteorological impact	Reference
Eastern China	May to Aug, 2019/2020	GEOS-Chem	GEOS-FP	–2.9 ppb	Yin et al., 2021
BTH				–1.4 ppb	
FWP				–3.2 ppb	
YRD				–3.2 ppb	
Eastern China		GEOS-Chem-XGBoost		–2.3 ppb	
BTH				–2.2 ppb	
FWP				–2.2 ppb	
YRD				–2.7 ppb	
Eastern and central China	Summer, 2013/2020	4-D meteorology-pollution decomposition model	World Meteorological Organization	Meteorology reduced the O_3 concentrations.	Lin et al., 2021
YRD	Apr to Sept, 2014–2018	KZ-MLR	CMA	Meteorology decreased (increased) O_3 from 2014 to the middle of 2016 (from the middle of 2016 to 2018)	Gao et al., 2021a
Eastern China	May, Jul, Sept, Dec, 2013/2017	WRF-Chem	FNL	–8.1 ~ +21.3 μg m^{-3}	Li et al., 2021
NCP	May 1st to Jun 10th, 2014–2019	MLR	FNL	+1.8 ppb yr^{-1}	Gao et al., 2021b
	Jun 11th to Jul 15th, 2014–2019			+2.4 ppb yr^{-1}	
	Jul 16th to Aug 31st, 2014–2019			–0.4 ppb yr^{-1}	
PRD (urban site)	2006–2019	MLR	ERA5	–0.04 ppb yr^{-1}	Li et al., 2022
PRD (regional site)				–0.11 ppb yr^{-1}	
Beijing	2013–2020	MLR	CMA, ERA5	+2.15 μg m^{-3} yr^{-1}	Gong et al., 2022

Region/City	Study period	Model	Meteorological data	Meteorological impact	Reference
Beijing	2015–2020	KZ-MLR	National Climatic Data Center	+45%	Zhang et al., 2022
Shenzhen				+20%	
Wuhan				+60%	
Nanjing				+75%	
YRD	Summer, 2015–2019	MLR	MERRA2	+5.0 μg m^{-3} yr^{-1}	Qian et al., 2022
Shanghai				+1.0 μg m^{-3} yr^{-1}	
Nanjing				+11.3 μg m^{-3} yr^{-1}	
Hangzhou				+1.9 μg m^{-3} yr^{-1}	
Heifei				+6.0 μg m^{-3} yr^{-1}	
BTH	Summer, 2015–2019	RF	ERA5	+0.74 ppb yr^{-1}	Weng et al., 2022
YRD				+1.35 ppb yr^{-1}	
PRD				–0.75 ppb yr^{-1}	
Sichuan				–0.91 ppb yr^{-1}	
BTH		Ridge regression		+0.54 ppb yr^{-1}	
YRD				+1.38 ppb yr^{-1}	
PRD				–1.13 ppb yr^{-1}	
Sichuan				–0.84 ppb yr^{-1}	
BTH		MLR		+0.55 ppb yr^{-1}	
YRD				+1.42 ppb yr^{-1}	
PRD				–1.1 ppb yr^{-1}	
Sichuan				–0.86 ppb yr^{-1}	
SCB	Apr to Aug, 2016/2019	WRF-CMAQ	FNL	+6.4 μg m^{-3}	Wu et al., 2022
	Jun to Aug, 2019/2020			–12.6 μg m^{-3}	
Tianjin	2015–2021	Lowess and RF	CMA	+2.1 μg m^{-3} yr^{-1}	Ding et al., 2023

Region/City	Study period	Model	Meteorological data	Meteorological impact	Reference
BTH	Summer, 2014–2021/2022	RF	ERA5	–0.02 ± 2.9 μg m^{-3}	Zheng et al., 2023
FWP				+7.23 ± 5.97 μg m^{-3}	
THB				+3.63 ± 4.51 μg m^{-3}	
PRD				–1.81 ± 2.14 μg m^{-3}	
SCB				+12.24 ± 4.07 μg m^{-3}	
YRD				+10.92 ± 3.24 μg m^{-3}	
Xiamen	2015–2020	KZ-MLR	ERA5	+2.71 μg m^{-3} yr^{-1}	Ji et al., 2023
Fuzhou				+2.17 μg m^{-3} yr^{-1}	
Longyan				+0.76 μg m^{-3} yr^{-1}	
Nanping				+1.78 μg m^{-3} yr^{-1}	
Northeast China	2013–2021	KZ-MLR	ERA5	+0.1688 μg m^{-3} yr^{-1}	Shang et al., 2023
Liaoning				–0.0864 μg m^{-3} yr^{-1}	
Jilin				+0.093 μg m^{-3} yr^{-1}	
Heilongjiang				+0.5562 μg m^{-3} yr^{-1}	
Eastern China	Apr to Sept, 2013/2020	WRF-CMAQ	FNL	+3.60 μg m^{-3}	Liu et al., 2023
BTH				+3.95 μg m^{-3}	
YRD				+3.91 μg m^{-3}	
FWP				+7.75 μg m^{-3}	
Beijing	2013–2020	Observation-based model	CMA	+0.52 ppb yr^{-1}	Pan et al., 2023
Chengdu				+0.57 ppb yr^{-1}	
Guangzhou				+0.59 ppb yr^{-1}	
Shanghai				+0.62 ppb yr^{-1}	
NCP	May to Aug, 2008/2009–2013	RegCM-Chem-YIBs	N/A	–0.88 ppb	Ma et al., 2023
FWP				–1.41 ppb	
YRD				–1.03 ppb	

Region/City	Study period	Model	Meteorological data	Meteorological impact	Reference
PRD	May to Aug, 2008/2009–2013	RegCM-Chem-YIBs	N/A	–0.23 ppb	Ma et al., 2023
SCB				–0.41 ppb	
NCP	May to Aug, 2008/2014–2018			–0.04 ppb	
FWP				–0.09 ppb	
YRD				–0.96 ppb	
PRD				–1.08 ppb	
SCB				+0.71 ppb	
NCP	Summer, 2015–2019	GEOS-Chem	MERRA2	+0.26 ppb yr^{-1}	Wang et al., 2024
		XGBoost		+0.19 ppb yr^{-1}	
		Deep learning model		+0.14 ppb yr^{-1}	
	Summer, 2019–2021	GEOS-Chem		–0.74 ppb yr^{-1}	
		XGBoost		–1.55 ppb yr^{-1}	
		Deep learning model		–1.74 ppb yr^{-1}	
China	2015–2022	KZ-XGBoost	ERA5	Meteorology increased O_3.	Yao et al., 2024
Eastern China	2019/2021	GEOS-Chem	MERRA2	–7.3 μg m^{-3}	Ni et al., 2024
		LightGBM		–6.8 μg m^{-3}	
BTH	2015–2022	XGBoost	ERA5	Meteorology led to a slight O_3 increase.	Luo et al., 2024
	Spring, 2015–2022 Summer, 2015–2022 Autumn, 2015–2022 Winter, 2015–2022			Meteorology increased O_3 by 8.2 μg m^{-3}/0.01 μg m^{-3}/2.7 μg m^{-3} in spring/summer/winter, and decreased O_3 by –0.3 μg m^{-3} in autumn.	
China	Summer, 2013–2022	MLR	ERA5	+0.2 μg m^{-3} yr^{-1}	Yan et al., 2024
BTH	Summer, 2013–2019			+0.9 μg m^{-3} yr^{-1}	
YRD				–0.3 μg m^{-3} yr^{-1}	

Region/City	Study period	Model	Meteorological data	Meteorological impact	Reference
BTH	Summer, 2019–2021	MLR	ERA5	–3.9 μg m^{-3} yr^{-1}	Yan et al., 2024
YRD				–4.1 μg m^{-3} yr^{-1}	
BTH	Summer, 2021–2022			+4.3 μg m^{-3} yr^{-1}	
YRD				+10.4 μg m^{-3} yr^{-1}	
YRD	2016–2023	KZ-MLR	ERA5	Meteorology decreased (increased) O_3 in 2016, 2020, 2021, 2023 (2017–2019, 2022).	Hu et al., 2024
	Spring, 2016–2023			Meteorology decreased (increased) O_3 in 2016, 2018, 2021, 2023 (2017, 2019, 2020, 2022).	
	Summer, 2016–2023			Meteorology decreased (increased) O_3 in 2020, 2021, 2023 (2016–2019, 2022).	
	Autumn, 2016–2023			Meteorology decreased (increased) O_3 in 2016–2017 (2018–2023).	
	Winter, 2016–2023			Meteorology decreased (increased)O_3 in 2018–2020, 2022 (2016, 2017, 2021, 2023).	
YRD	Spring, 2014/2020	WRF-Chem	FNL	–0.89 ppb	Li et al., 2024
	Summer, 2014/2020			+0.23 ppb	
	Autumn, 2014/2020			–2.74 ppb	
	Winter, 2014/2020			–3.86 ppb	
PRD	Spring, 2013–2022	MLR	ERA5	+0.88 ppb yr^{-1}	Cao et al., 2024
YRD	2015–2022	KZ-MLR	ERA5	The meteorological impacts account for an average of 71.8% of O_3	Wu and An, 2025

[a] Symbol "–" means the continuous study period from the start year to the end year (left of –) to the end year (right of –); Symbol "/" means the discrete study period.

[b] The meteorological impact expressed by ppb yr^{-1} or μg m^{-3} yr^{-1} means the trend from the start to the end year of the study period. Meteorological impact expressed by ppb, μg m^{-3}, or % means the difference between the end year and start year (end year – start year).

Table S2. Summary of the meteorological variables from the ERA5, MERRA2, FNL, and FNL025 reanalysis datasets used to establish MLR models.

Abbreviations	Description	Meteorological Dataset
SLP	Daily mean sea level pressure (hPa)	ERA5, MERRA2, FNL, FNL025
TCCday	Total cloud area fraction (%) averaged over 08:00 to 17:00 LT	ERA5, MERRA2
PBLHday	Planetary boundary layer height (m) averaged over 08:00 to 17:00 LT	ERA5, MERRA2, FNL, FNL025
U10	Daily mean 10-meter eastward wind (m s^{-1})	ERA5, MERRA2, FNL, FNL025
V10	Daily mean 10-meter northward wind (m s^{-1})	ERA5, MERRA2, FNL, FNL025
T2max	Daily maximum 2-meter air temperature (℃)	ERA5, MERRA2, FNL, FNL025
SSRDday	Surface incoming shortwave flux (W m^{-2}) averaged over 08:00 to 17:00 LT	ERA5, MERRA2
TP	Total precipitation (mm day^{-1})	ERA5, MERRA2
PWAT	Daily mean precipitable water considered as a single layer (mm)	FNL, FNL025
RH2	Daily mean 2-meter relative humidity (%)	ERA5, MERRA2, FNL, FNL025
V850	Daily mean northward wind at 850 hPa (m s^{-1})	ERA5, MERRA2, FNL, FNL025

Table S3. Comparison of meteorology-driven MDA8 O_3 trends (ppb yr^{-1}) derived from multiple linear regression (MLR), random forest (RF), and GEOS-Chem (GC) models using different model performance criteria (the R^2 of the RF model ≥ 0.5, 0.6, and 0.4) across seasons and regions.

Season	R^2	Available stations [a]	China				BTH				YRD				PRD			
			MLR	RF	GC	CV [b]	MLR	RF	GC	CV	MLR	RF	GC	CV	MLR	RF	GC	CV
Spring	$R^2 \geq 0.5$	1162	+0.48	+0.15	+0.14	0.75	+0.26	–0.01	+0.12	1.06	+0.80	+0.25	+0.37	0.61	+0.94	+0.78	+0.77	0.11
	$R^2 \geq 0.6$	882	+0.50	+0.14	+0.14	0.81	+0.26	–0.00	+0.12	1.07	+0.86	+0.25	+0.37	0.66	+0.89	+0.75	+0.77	0.10
	$R^2 \geq 0.4$	1250	+0.47	+0.16	+0.14	0.73	+0.26	–0.01	+0.12	1.06	+0.77	+0.25	+0.36	0.60	+0.89	+0.75	+0.77	0.09
Summer	$R^2 \geq 0.5$	1059	+0.23	+0.01	–0.03	2.00	+0.03	–0.16	–0.18	1.08	+0.45	+0.25	+0.40	0.29	+0.07	+0.13	+0.10	0.32
	$R^2 \geq 0.6$	642	+0.31	+0.02	–0.01	1.69	+0.06	–0.20	–0.17	1.40	+0.51	+0.21	+0.34	0.42	+0.08	+0.13	+0.10	0.25
	$R^2 \geq 0.4$	1223	+0.20	+0.00	–0.04	2.39	+0.04	–0.15	–0.19	1.24	+0.43	+0.25	+0.39	0.27	+0.06	+0.13	+0.09	0.34
Autumn	$R^2 \geq 0.5$	1203	+0.15	+0.34	+0.03	0.88	–0.27	+0.19	–0.13	3.38	+0.37	+0.53	+0.24	0.38	+0.83	+0.81	+0.53	0.23
	$R^2 \geq 0.6$	1041	+0.18	+0.36	+0.04	0.85	–0.27	+0.19	–0.14	3.40	+0.40	+0.55	+0.24	0.39	+0.85	+0.83	+0.54	0.23
	$R^2 \geq 0.4$	1252	+0.15	+0.33	+0.03	0.90	–0.27	+0.19	–0.13	3.38	+0.36	+0.52	+0.24	0.38	+0.83	+0.81	+0.53	0.23
Winter	$R^2 \geq 0.5$	1094	+0.30	+0.12	+0.25	0.40	+0.26	+0.13	+0.09	0.55	+0.19	+0.06	+0.27	0.59	+0.72	+0.64	+0.72	0.07
	$R^2 \geq 0.6$	738	+0.33	+0.13	+0.24	0.41	+0.26	+0.13	+0.10	0.53	+0.20	+0.06	+0.27	0.59	+0.70	+0.66	+0.73	0.05
	$R^2 \geq 0.4$	1217	+0.28	+0.12	+0.25	0.40	+0.26	+0.13	+0.10	0.55	+0.17	+0.06	+0.27	0.62	+0.70	+0.63	+0.72	0.07

[a] "Available stations" denotes the number of state-controlled monitoring stations with the R^2 of the Random Forest model of ≥ 0.5, 0.6, and 0.4.

[b] The absolute value of the coefficient of variation (CV) is calculated by the standard deviation of the trends derived from MLR, RF, and GC models divided by the mean.

Table S4. The 10-year trend in each meteorological factor used to establish MLR models from the ERA5, MERRA2, and FNL during four seasons.

Season	Dataset	RH2 (% yr^{-1})	U10 (m s^{-1} yr^{-1})	V10 (m s^{-1} yr^{-1})	SSRDday (W m^{-2} yr^{-1})	PBLHday (m yr^{-1})	TCCday (% yr^{-1})	TP (mm day^{-1} yr^{-1}) or PWAT (mm yr^{-1})	SLP (hPa yr^{-1})	T2max (°C yr^{-1})	V850 (m s^{-1} yr^{-1})
Spring	ERA5	+0.08	+0.01	–0.00	+0.68	+3.89	+0.00	–0.02	–0.02	+0.18	–0.01
	MERRA2	+0.33	+0.01	–0.00	+1.59	+5.54	+0.24	+0.02	–0.08	+0.16	+0.00
	FNL	+0.12	+0.01	–0.01	/	+14.44	/	+0.20	–0.09	+0.12	–0.01
Summer	ERA5	+0.18	–0.00	+0.01	–0.72	–2.10	+0.18	+0.03	+0.02	+0.08	+0.03
	MERRA2	+0.35	+0.00	+0.03	+1.11	–6.95	+0.29	–0.03	–0.04	+0.04	+0.05
	FNL	+0.29	–0.00	+0.01	/	+4.96	/	+0.23	–0.08	–0.01	+0.05
Autumn	ERA5	–0.17	+0.01	–0.02	–1.62	+0.04	–0.21	–0.04	+0.21	–0.10	–0.05
	MERRA2	+0.11	+0.00	–0.03	–0.99	–2.52	–0.17	–0.06	+0.17	–0.12	–0.04
	FNL	–0.29	+0.00	–0.03	/	+6.66	/	–0.15	+0.13	–0.16	–0.05
Winter	ERA5	+0.07	+0.00	–0.00	–0.03	+2.71	+0.41	+0.00	+0.04	+0.02	+0.03
	MERRA2	+0.36	–0.01	–0.01	+0.68	+5.29	+0.31	+0.01	+0.00	+0.04	+0.04
	FNL	+0.15	–0.01	–0.01	/	+8.68	/	+0.12	–0.03	+0.01	+0.03

Table S5. Trends in simulated (Sim) and observed (Obs) monthly mean MDA8 O_3 concentrations (ppb yr^{-1}) during 2013–2022, 2013–2017, and 2018–2022.

Region / Time period	China		BTH		YRD		PRD	
	Sim	Obs	Sim	Obs	Sim	Obs	Sim	Obs
2013–2022	–0.05	+0.84	–0.11	+0.89	+0.40	+0.97	+0.39	+1.07
2013–2017	–0.84	+0.27	–0.82	+0.22	–0.40	+0.29	+0.22	+0.31
2018–2022	–1.78	–0.86	–2.86	–2.49	–2.00	–0.96	–1.38	+0.17

Reference

Cao, T., Wang, H., Chen, X., Li, L., Lu, X., Lu, K., and Fan, S.: Rapid increase in spring ozone in the Pearl River Delta, China during 2013-2022, npj Clim. Atmos. Sci., 7, 309, https://doi.org/10.1038/s41612-024-00847-3, 2024.

Chen, L., Zhu, J., Liao, H., Yang, Y., and Yue, X.: Meteorological influences on $PM_{2.5}$ and O_3 trends and associated health burden since China's clean air actions, Sci. Total Environ., 744, 140837, https://doi.org/10.1016/j.scitotenv.2020.140837, 2020.

Dang, R., Liao, H., and Fu, Y.: Quantifying the anthropogenic and meteorological influences on summertime surface ozone in China over 2012–2017, Sci. Total Environ., 754, 142394, https://doi.org/10.1016/j.scitotenv.2020.142394, 2021.

Ding, D., Xing, J., Wang, S., Chang, X., and Hao, J.: Impacts of emissions and meteorological changes on China's ozone pollution in the warm seasons of 2013 and 2017, Front. Environ. Sci. Eng., 13, https://doi.org/10.1007/s11783-019-1160-1, 2019.

Ding, J., Dai, Q., Fan, W., Lu, M., Zhang, Y., Han, S., and Feng, Y.: Impacts of meteorology and precursor emission change on O_3 variation in Tianjin, China from 2015 to 2021, J. Environ. Sci., 126, 506–516, https://doi.org/10.1016/j.jes.2022.03.010, 2023.

Gao, D., Xie, M., Liu, J., Wang, T., Ma, C., Bai, H., Chen, X., Li, M., Zhuang, B., and Li, S.: Ozone variability induced by synoptic weather patterns in warm seasons of 2014–2018 over the Yangtze River Delta region, China, Atmos. Chem. Phys., 21, 5847–5864, https://doi.org/10.5194/acp-21-5847-2021, 2021a.

Gao, L., Wang, T., Ren, X., Ma, D., Zhuang, B., Li, S., Xie, M., Li, M., and Yang, X.-Q.: Subseasonal characteristics and meteorological causes of surface O_3 in different East Asian summer monsoon periods over the North China Plain during 2014–2019, Atmos. Environ., 264, 118704, https://doi.org/10.1016/j.atmosenv.2021.118704, 2021b.

Gong, S., Zhang, L., Liu, C., Lu, S., Pan, W., and Zhang, Y.: Multi-scale analysis of the impacts of meteorology and emissions on $PM_{2.5}$ and O_3 trends at various regions in China from 2013 to 2020 2. Key weather elements and emissions, Sci. Total Environ., 824, 153847, https://doi.org/10.1016/j.scitotenv.2022.153847, 2022.

Han, H., Liu, J., Shu, L., Wang, T., and Yuan, H.: Local and synoptic meteorological influences on daily variability in summertime surface ozone in eastern China, Atmos. Chem. Phys., 20, 203–

222, https://doi.org/10.5194/acp-20-203-2020, 2020.

Hu, F., Xie, P., Xu, J., Lv, Y., Zhang, Z., Zheng, J., and Tian, X.: Long-term trends of ozone in the Yangtze River Delta, China: spatiotemporal impacts of meteorological factors, local, and non-local emissions, J. Environ. Sci., S1001074224003826, https://doi.org/10.1016/j.jes.2024.07.017, 2024.

Ji, X., Hong, Y., Lin, Y., Xu, K., Chen, G., Liu, T., Xu, L., Li, M., Fan, X., Wang, H., Zhang, H., Chen, Y., Yang, C., Lin, Z., and Chen, J.: Impacts of Synoptic Patterns and Meteorological Factors on Distribution Trends of Ozone in Southeast China During 2015–2020, J. Geophys. Res.: Atmos., 128, e2022JD037961, https://doi.org/10.1029/2022JD037961, 2023.

Li, K., Jacob, D. J., Shen, L., Lu, X., De Smedt, I., and Liao, H.: Increases in surface ozone pollution in China from 2013 to 2019: anthropogenic and meteorological influences, Atmos. Chem. Phys., 20, 11423–11433, https://doi.org/10.5194/acp-20-11423-2020, 2020.

Li, M., Wang, T., Shu, L., Qu, Y., Xie, M., Liu, J., Wu, H., and Kalsoom, U.: Rising surface ozone in China from 2013 to 2017: a response to the recent atmospheric warming or pollutant controls?, Atmos. Environ., 246, 118130, https://doi.org/10.1016/j.atmosenv.2020.118130, 2021.

Li, X., Yuan, B., Parrish, D. D., Chen, D., Song, Y., Yang, S., Liu, Z., and Shao, M.: Long-term trend of ozone in southern China reveals future mitigation strategy for air pollution, Atmos. Environ., 269, 118869, https://doi.org/10.1016/j.atmosenv.2021.118869, 2022.

Li, Y., Wang, T., Wang, Q., Li, M., Qu, Y., Wu, H., and Xie, M.: Exploring the role of aerosol-ozone interactions on O_3 surge and $PM_{2.5}$ decline during the clean air action period in Eastern China 2014–2020, Atmos. Res., 302, 107294, https://doi.org/10.1016/j.atmosres.2024.107294, 2024.

Lin, C., Lau, A. K. H., Fung, J. C. H., Song, Y., Li, Y., Tao, M., Lu, X., Ma, J., and Lao, X. Q.: Removing the effects of meteorological factors on changes in nitrogen dioxide and ozone concentrations in China from 2013 to 2020, Sci. Total Environ., 793, 148575, https://doi.org/10.1016/j.scitotenv.2021.148575, 2021.

Liu, Y. and Wang, T.: Worsening urban ozone pollution in China from 2013 to 2017 – part 1: the complex and varying roles of meteorology, Atmos. Chem. Phys., 20, 6305–6321, https://doi.org/10.5194/acp-20-6305-2020, 2020.

Liu, Y., Geng, G., Cheng, J., Liu, Y., Xiao, Q., Liu, L., Shi, Q., Tong, D., He, K., and Zhang, Q.:

Drivers of Increasing Ozone during the Two Phases of Clean Air Actions in China 2013–2020, Environ. Sci. Technol., 57, 8954–8964, https://doi.org/10.1021/acs.est.3c00054, 2023.

Luo, Z., Lu, P., Chen, Z., and Liu, R.: Ozone Concentration Estimation and Meteorological Impact Quantification in the Beijing-Tianjin-Hebei Region Based on Machine Learning Models, Earth Space Sci., 11, e2023EA003346, https://doi.org/10.1029/2023EA003346, 2024.

Ma, D., Wang, T., Wu, H., Qu, Y., Liu, J., Liu, J., Li, S., Zhuang, B., Li, M., and Xie, M.: The effect of anthropogenic emission, meteorological factors, and carbon dioxide on the surface ozone increase in China from 2008 to 2018 during the East Asia summer monsoon season, Atmos. Chem. Phys., 23, 6525–6544, https://doi.org/10.5194/acp-23-6525-2023, 2023.

Mousavinezhad, S., Choi, Y., Pouyaei, A., Ghahremanloo, M., and Nelson, D. L.: A comprehensive investigation of surface ozone pollution in China, 2015–2019: separating the contributions from meteorology and precursor emissions, Atmos. Res., 257, 105599, https://doi.org/10.1016/j.atmosres.2021.105599, 2021.

Ni, Y., Yang, Y., Wang, H., Li, H., Li, M., Wang, P., Li, K., and Liao, H.: Contrasting changes in ozone during 2019–2021 between eastern and the other regions of China attributed to anthropogenic emissions and meteorological conditions, Sci. Total Environ., 908, 168272, https://doi.org/10.1016/j.scitotenv.2023.168272, 2024.

Pan, W., Gong, S., Lu, K., Zhang, L., Xie, S., Liu, Y., Ke, H., Zhang, X., and Zhang, Y.: Multi-scale analysis of the impacts of meteorology and emissions on $PM_{2.5}$ and O_3 trends at various regions in China from 2013 to 2020 3. Mechanism assessment of O_3 trends by a model, Sci. Total Environ., 857, 159592, https://doi.org/10.1016/j.scitotenv.2022.159592, 2023.

Qian, J., Liao, H., Yang, Y., Li, K., Chen, L., and Zhu, J.: Meteorological influences on daily variation and trend of summertime surface ozone over years of 2015–2020: Quantification for cities in the Yangtze River Delta, Sci. Total Environ., 834, 155107, https://doi.org/10.1016/j.scitotenv.2022.155107, 2022.

Shang, N., Gui, K., Zhao, H., Yao, W., Zhao, H., Zhang, X., Zhang, X., Li, L., Zheng, Y., Wang, Z., Wang, Y., Che, H., and Zhang, X.: Decomposition of meteorological and anthropogenic contributions to near-surface ozone trends in Northeast China (2013–2021), Atmos. Pollut. Res., 14, 101841, https://doi.org/10.1016/j.apr.2023.101841, 2023.

Sun, L., Xue, L., Wang, Y., Li, L., Lin, J., Ni, R., Yan, Y., Chen, L., Li, J., Zhang, Q., and Wang, W.:

Impacts of meteorology and emissions on summertime surface ozone increases over central eastern China between 2003 and 2015, Atmos. Chem. Phys., 19, 1455–1469, https://doi.org/10.5194/acp-19-1455-2019, 2019.

Sun, Y., Yin, H., Lu, X., Notholt, J., Palm, M., Liu, C., Tian, Y., and Zheng, B.: The drivers and health risks of unexpected surface ozone enhancements over the Sichuan Basin, China, in 2020, Atmos. Chem. Phys., 21, 18589–18608, https://doi.org/10.5194/acp-21-18589-2021, 2021.

Wang, M., Chen, X., Jiang, Z., He, T.-L., Jones, D., Liu, J., and Shen, Y.: Meteorological and anthropogenic drivers of surface ozone change in the North China Plain in 2015–2021, Sci. Total Environ., 906, 167763, https://doi.org/10.1016/j.scitotenv.2023.167763, 2024.

Wang, P., Guo, H., Hu, J., Kota, S. H., Ying, Q., and Zhang, H.: Responses of $PM_{2.5}$ and O_3 concentrations to changes of meteorology and emissions in China, Sci. Total Environ., 662, 297–306, https://doi.org/10.1016/j.scitotenv.2019.01.227, 2019.

Weng, X., Forster, G. L., and Nowack, P.: A machine learning approach to quantify meteorological drivers of ozone pollution in China from 2015 to 2019, Atmos. Chem. Phys., 22, 8385–8402, https://doi.org/10.5194/acp-22-8385-2022, 2022.

Wu, K., Wang, Y., Qiao, Y., Liu, Y., Wang, S., Yang, X., Wang, H., Lu, Y., Zhang, X., and Lei, Y.: Drivers of 2013–2020 ozone trends in the Sichuan Basin, China: impacts of meteorology and precursor emission changes, Environ. Pollut., 300, 118914, https://doi.org/10.1016/j.envpol.2022.118914, 2022.

Wu, L. and An, J.: Quantitative impacts of meteorology and emissions on the long-term trend of O_3 in the YRD, China from 2015 to 2022, J. Environ. Sci., 149, 314–329, https://doi.org/10.1016/j.jes.2024.01.038, 2025.

Yan, D., Jin, Z., Zhou, Y., Li, M., Zhang, Z., Wang, T., Zhuang, B., Li, S., and Xie, M.: Anthropogenically and meteorologically modulated summertime ozone trends and their health implications since China’s clean air actions, Environ. Pollut., 343, 123234, https://doi.org/10.1016/j.envpol.2023.123234, 2024.

Yang, J., Liu, J., Han, S., Yao, Q., and Cai, Z.: Study of the meteorological influence on ozone in urban areas and their use in assessing ozone trends in all seasons from 2009 to 2015 in Tianjin, China, Meteorol. Atmos. Phys., 131, 1661–1675, https://doi.org/10.1007/s00703-019-00664-x, 2019a.

Yang, L., Luo, H., Yuan, Z., Zheng, J., Huang, Z., Li, C., Lin, X., Louie, P. K. K., Chen, D., and Bian, Y.: Quantitative impacts of meteorology and precursor emission changes on the long-term trend of ambient ozone over the Pearl River Delta, China, and implications for ozone control strategy, Atmos. Chem. Phys., 19, 12901–12916, https://doi.org/10.5194/acp-19-12901-2019, 2019b.

Yao, S., Wei, W., Cheng, S., Niu, Y., and Guan, P.: Impacts of meteorology and emissions on O_3 pollution during 2013–2018 and corresponding control strategy for a typical industrial city of China, Atmosphere, 12, 619, https://doi.org/10.3390/atmos12050619, 2021.

Yao, T., Ye, H., Wang, Y., Zhang, J., Guo, J., and Li, J.: Kolmogorov-Zurbenko filter coupled with machine learning to reveal multiple drivers of surface ozone pollution in China from 2015 to 2022, Sci. Total Environ., 949, 175093, https://doi.org/10.1016/j.scitotenv.2024.175093, 2024.

Yin, H., Lu, X., Sun, Y., Li, K., Gao, M., Zheng, B., and Liu, C.: Unprecedented decline in summertime surface ozone over eastern China in 2020 comparably attributable to anthropogenic emission reductions and meteorology, Environ. Res. Lett., 16, 124069, https://doi.org/10.1088/1748-9326/ac3e22, 2021.

Yu, Y., Wang, Z., He, T., Meng, X., Xie, S., and Yu, H.: Driving factors of the significant increase in surface ozone in the Yangtze River Delta, China, during 2013–2017, Atmos. Pollut. Res., 10, 1357–1364, https://doi.org/10.1016/j.apr.2019.03.010, 2019.

Zhang, Y., Lei, R., Cui, S., Wang, H., Chen, M., and Ge, X.: Spatiotemporal trends and impact factors of $PM_{2.5}$ and O_3 pollution in major cities in China during 2015–2020, Chin. Sci. Bull., 67, 2029–2042, https://doi.org/10.1360/TB-2021-0767, 2022.

Zhao, N., Wang, G., Li, G., and Lang, J.: Trends in Air Pollutant Concentrations and the Impact of Meteorology in Shandong Province, Coastal China, during 2013-2019, Aerosol Air Qual. Res., 21, 200545, https://doi.org/10.4209/aaqr.200545, 2021.

Zheng, H., Kong, S., He, Y., Song, C., Cheng, Y., Yao, L., Chen, N., and Zhu, B.: Enhanced ozone pollution in the summer of 2022 in China: the roles of meteorology and emission variations, Atmos. Environ., 301, 119701, https://doi.org/10.1016/j.atmosenv.2023.119701, 2023.